

# Moisture Effect on the Low- and High-Temperature Dielectric Relaxations in Nylon-6

E. LAREDO, M. C. HERNANDEZ

Physics Department, Universidad Simón Bolívar, Apartado 89.000, Caracas 1081, Venezuela

Received 12 May 1997; revised 25 July 1997; accepted 30 July 1997

**ABSTRACT:** The effect of water sorption on the dielectric relaxation processes of nylon-6 samples with water concentrations ranging from the dry to the water-saturated polymer has been studied by thermally stimulated depolarization currents experiments in a broad temperature range, from 77 to 365 K. The strengths of the low-temperature modes,  $\gamma$ - and  $\beta$ -peaks, are affected in opposite ways by the water concentration,  $h$ , as the first one shows a decrease in intensity and the second one grows as  $h$  increases. The precise determination of the relaxation parameters is made by the decomposition in elementary Debye processes and best fitting to the experimental profile of the complex peak. For  $h < 3\%$ , the reorienting energies are almost independent of the water content, and the most significant intensity variations occur. The firmly bound water is held responsible for these effects. As for the higher temperature zone besides the  $\alpha$ -peak, which is the dielectric manifestation of the glass transition, intermediate temperatures modes are observed at high  $h$  values and are originated by the loosely bound water, while the highest temperature peak is attributed to a Maxwell–Wagner interfacial polarization. The characteristic parameters of the  $\alpha$ -mode are determined and related to the plasticization effect of water. © 1997 John Wiley & Sons, Inc. *J Polym Sci B: Polym Phys* **35**: 2879–2888, 1997

**Keywords:** nylon-6; dry and water saturated; thermally stimulated depolarization current; dielectric relaxation; glass transition; water sorption

## INTRODUCTION

Water sorption in polyamides has been extensively studied, and its effect on the dielectric properties of the material has been followed mainly by dielectric constant experiments since 1959.<sup>1–5</sup> Moisture in these materials has a strong effect on their dielectric properties because of the existence of interchain H-bonding sites between two amide groups which are present in the chemical structure of the material. As a result of the sorption of water molecules, the mobility of the molecular segments and/or the number of orientable ones are altered, resulting in significant changes in the low-temperature  $\gamma$ - and  $\beta$ -modes and on the

$\alpha$ -relaxation, which is the manifestation of the glass–rubber transition. These three relaxation modes have been detected by dynamic mechanical analysis (DMA),<sup>6–10</sup> dielectric spectroscopy (DS)<sup>1–5</sup> as a function of temperature and frequency, and thermally stimulated currents (TSDC) experiments.<sup>11–14</sup>

Several interpretations referring to the specific molecular motions that originate these relaxations have been proposed on the basis of the water sorption mechanism. It is generally accepted that water enters in different forms in nylons. Puffr and Sebenda<sup>15</sup> proposed a sorption model in the moisture-accessible regions of nylon-6, where three water molecules are sorbed on two close amide groups, which were initially H-bound to two other amide groups. The first one binds the two carbonyl oxygens of the two neighboring amide groups through a double H bond, and it is termed

Correspondence to: E. Laredo (Email: elaredo@usb.ve)

*Journal of Polymer Science: Part B: Polymer Physics*, Vol. 35, 2879–2888 (1997)  
© 1997 John Wiley & Sons, Inc. CCC 0887-6266/97/172879-10

as tightly bound water, as in this step a large amount of energy is evolved; this stage goes up to a concentration of one water molecule per two amide groups in the amorphous regions. In a second stage, three water molecules per two amide groups, the remaining two water molecules will join the already existing H bonds between the CO of one amide group and the NH of another; this mechanism results in loosely bound water as the thermal effect is negligible. Starkweather<sup>2</sup> calculated that, above one water molecule per two amide groups in the amorphous regions, water form clusters; near saturation the average cluster size is around three water molecules. However, many of the early interpretations on the effect of moisture on the low-temperature relaxations assigned them to the motion of chain segments including amide groups which were not H-bound to neighboring chains;<sup>6</sup> i.e. water is not involved in the motion responsible for the  $\beta$ -relaxation. Additionally, the  $\gamma$ -relaxation was thought to be due to the combined motion of amide and methylene groups.

Patmanathan et al.<sup>5</sup> studied the variation of the dielectric spectrum of dry and saturated nylon-12 and concluded that the localized  $\gamma$ - and  $\beta$ -modes, which vary in opposite ways with the water content, are due to the plasticization effect of water. The  $\beta$ -relaxation is attributed to the motion of molecular segments and of water molecules located in the amorphous zones where they form H bonds with the CO and NH groups. They propose that the mechanism responsible for the  $\gamma$ -relaxation includes motions of the amide group. Additionally, an increase in the density of the nylon-12 samples was observed on going from the dry to the humid state. The interpretation offered consists in assuming that water molecules in nylons occupy vacant sites in the loosely chains packed in the amorphous regions. The plasticization effect of water, clearly observed by the shift of the  $\alpha$ -relaxation to lower temperatures, is explained by an increase in the probability of breaking H bonds. An alternative explanation by Starkweather and Barkley<sup>2</sup> is that the introduction of a water molecule between two amide groups in nylon-6,6, by breaking the existing H bond, allows a more efficient chain packing as the steric requirements for the formation of H bonds are now suppressed. Cluster formation of water molecules has also been proposed, as additional water molecules would be attached to the initial molecules loosely or firmly bound to the polymer segments. However, the specific molecular processes which

originate the low-temperature relaxations, based on poorly resolved spectra, are difficult to identify.

Experimental results from the thermally stimulated depolarization current technique (TSDC) show much better resolved spectra which can be analyzed in more detail. Ikeda and Matsuda's<sup>12</sup> TSDC results on nylon-6, below room temperature, are interpreted by setting a temperature of 208 K for the onset of the plasticization effect. For  $T < 208$  K the effect of water molecules is explained as a reduction in the number of free NH and CO groups due to the H bond they form with water. The most recent TSDC work on nylon-6 by Frank et al.<sup>14</sup> deals with the moisture effect on the low-temperature part of the spectrum, i.e. the  $\gamma$ - and  $\beta$ -relaxations. The authors explain the variations observed on the  $\gamma$ -relaxation by the reorientation process of firmly bound water, while the loosely bound one will be responsible for the variations of the  $\beta$  relaxation. Water in clusters at high humidity contents is also assumed.

In this work, we present results of water sorption on the low-temperature  $\gamma$ - and  $\beta$ -relaxations of nylon-6, as well as the detailed TSDC study of the  $\alpha$ -relaxation which is attributed to the onset of large scale cooperative motions which occur at the glass transition temperature. The complex low- and high-temperature TSDC spectra (from 77 to 280 K and from 280 to 370 K, respectively), will be analyzed in detail with the powerful direct signal analysis (DSA),<sup>16</sup> which allows a precise determination of the number of modes existing under each band, and the relaxation parameters, i.e. reorientation energy and inverse frequency factor,  $\tau_0$  of each process as a function of the water concentration in weight,  $h$ . The plasticization effect of water will in this way be followed quantitatively for  $0.1\% \leq h \leq 10.0\%$ . By the study of the whole relaxation TSDC spectrum a better understanding of the effect of moisture sorption is reached, and the possible origins of the observed relaxation modes are discussed.

## EXPERIMENTAL

### Materials

The nylon-6 (ADS40) used in this work came from SNIA, Milan, Italy. Its weight average molecular weight is  $\bar{M}_w = 62,000$  g/mol. Films are obtained by compression molding at 493 K and 2000 psi. The average thickness is 400  $\mu\text{m}$ . Finally, 20 mm diameter disks were cut from them. The crys-

tallinity degree ( $X_c$ ) is determined from the area of the melting peak at 492 K obtained by differential scanning calorimetry at a heating rate of 10 K/min in a Perkin-Elmer DSC-7.  $X_c = 42\%$  for the samples used here; this value is calculated by using 6.6 kJ/mol as the heat of fusion for a 100% crystalline nylon-6.

The weight concentration of water molecules,  $h$ , is defined as the mass increase of the humid material divided by the mass of the dry sample, and it is determined by weighting the sample before each experiment. The starting wet sample is obtained by immersion in distilled water for 24 h at room temperature. A value of  $h = 12.3\%$  is estimated for the water-saturated nylon-6 sample. The number of water molecules absorbed per accessible amide group in the amorphous regions can be calculated by multiplying  $h$  by 0.11. For the study of the effect of water molecules on the low-temperature relaxation modes the drying procedure was carried out by keeping the sample under dynamic vacuum at a pressure of  $2 \times 10^{-6}$  Torr and 294 K. The sample was not taken to temperatures higher than room temperature for this series of experiments. When the variation of the  $\alpha$ -peak with water moisture is studied, the drying process is due to the degassing of the material and to the effect of the temperatures reached during the TSDC runs and polarization steps. The  $h$  values reported here were determined by repeating all the thermal treatments performed in the realization of the series of TSDC runs. The sample was weighted before each current recording, i.e. after the corresponding simulated polarization step. The sensitivity of our gravimetric determination is 0.1 mg.

### TSDC Experiments

TSDC experiments are performed in a cell and measuring system designed in our laboratory. The sample is located in the TSDC measuring cell between two vertical metallic disks lightly spring loaded that are the plates of a capacitor. The cell, carefully evacuated ( $2 \times 10^{-6}$  Torr), is then filled with dry nitrogen (600 Torr) for the duration of the polarization step. The perturbation is in this case the electric polarizing field,  $E_p$ , typically 500 kV m<sup>-1</sup>, that is applied at the temperature,  $T_p$ , during a time  $t_p$ , typically 3 min, long enough to orient the species under study to saturation. Then the sample is quenched rapidly (0.9 K s<sup>-1</sup>) to liquid nitrogen temperature (LNT). The field is switched off, and the cell is evacuated to  $2 \times 10^{-6}$

Torr and filled with dry helium (100 Torr), which acts as an interchange gas. The depolarization current is measured with a Keithley 642 electrometer, as a function of temperature, which increases at a constant rate,  $b = 0.07$  K s<sup>-1</sup>. The sensitivity of our system is  $10^{-16}$  A, and the signal to noise ratio is close to 500. The analog output of the electrometer is read by a voltmeter-scanner as well as the temperature and elapsed time. The experiment is completely automated, and these variables are stored in a computer file for subsequent analysis. The different current peaks can be isolated by choosing the polarization temperature at the peak maximum,  $T_M$ , and by partially discharging (peak cleaning) the low-temperature side of the TSDC complex peak. All the low-temperature spectra shown in this work are polarized at 246 K. For the  $\alpha$ -transition study, the polarization temperature for the complex spectra is above or at the temperature of the peak maximum. The cleaning procedure is performed in each case by partially discharging the  $\alpha$ -mode polarized at the temperature of the current maximum,  $T_{M\alpha}$ , up to a temperature equal to  $T_{M\alpha} - 15$  K.

## ANALYSIS PROCEDURE

### Analysis of the TSDC Peaks

The direct signal analysis is a fitting procedure, and its application to the complex TSDC peaks has been recently described and discussed in great detail.<sup>16</sup> The method consists in finding the  $N$  elementary curves whose characteristic energies are equally spaced in a given energy window and whose combination best fits the whole experimental TSDC profile. The recorded TSDC current density is approximated by

$$J_D(T_j) = \sum_{i=1}^N \frac{P_{0i}(T_j)}{\tau_i(T_j)} \exp\left(-\frac{1}{b_h} \int_{T_0}^{T_j} \frac{dT'}{\tau_i(T')}\right) \quad j = 1, M; \quad N \leq M/2 \quad (1)$$

where  $\tau_i(T)$  is the relaxation time for each elementary process,  $P_{0i}(T)$  is its contribution to the total polarization, and  $b_h$  is the heating rate. The temperature dependence for the relaxation time can be either Arrhenius, adequate for low-temperature relaxations in polymers (below  $T_g$ )

$$\tau(T) = \tau_0 \exp(E/kT) \quad (2)$$

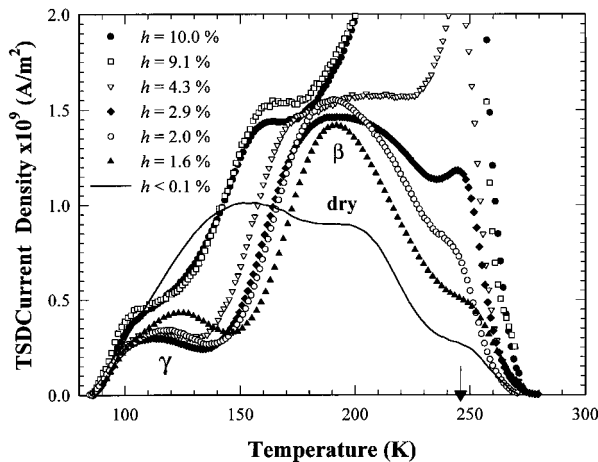


**Figure 1.** Low-temperature TSDC spectra of nylon-6:  $\gamma$ - and  $\beta$ -relaxations.  $T_p = 246$  K.

or Vogel–Tammann–Fulcher, VTF, which is satisfactory for relaxations occurring at temperatures around and above  $T_g$ :

$$\tau(T) = \tau_0 \exp(E/k(T - T_\infty)) \quad (3)$$

In this case  $T_\infty$  is the critical temperature at which molecular motions in the material become infinitely slow.

In the DSA method,  $J_D(T)$  is adjusted to the experimental data using the Marquardt–Levenberg nonlinear least-squares algorithm. The input parameters are the threshold and width of the energy window and the number of adjacent bins,  $N$ . The adjusted parameters are the  $\tau_{0i}$ 's and the  $P_{0i}$ 's. Initially we choose a box-shaped distribution for  $P_{0i}$ , i.e., every bin contributes equally to the total polarization of the sample, and a suitable set of  $\tau_{0i}$ 's. The results of the fitting procedure can be summarized in an energy histogram which covers the selected energy window divided in  $N$  energy bins and whose height,  $P_{0i}$ , is proportional to the area under the curve corresponding to each elementary process. The program also fits the  $T_\infty$  value when VTF relaxation times are selected. It has been shown that the procedure works very well for  $\beta$  relaxations ( $T_\beta < T_g$ ) in polycarbonate,<sup>17</sup> tyrosine-derived polycarbonates,<sup>18</sup> and thermotropic polyesters.<sup>19,20</sup> All these  $\beta$ -relaxations were fitted by using an Arrhenius temperature dependence for the relaxation times. The fitting for  $\alpha$ -relaxation has been successfully performed on polycarbonate<sup>17</sup> and diethyl maleate functionalized linear low-density polyethylene,<sup>21</sup> and convergence is achieved only when VTF relax-

ation times are used. This temperature dependence has been shown in a great number of works to be adequate for transitions at  $T \geq T_g$ , and it has received a plausible basis by using either the concept of free volume<sup>22</sup> or statistical thermodynamics.<sup>23</sup>

## RESULTS AND DISCUSSION

### Low-Temperature Relaxations ( $\gamma$ - and $\beta$ -Modes)

In Figures 1 and 2 the variation of the low-temperature TSDC spectrum ( $T < 280$  K) is plotted for various moisture contents. The first graph corresponds to the whole  $h$  range, and the second one corresponds to  $h \leq 1.6\%$ , which is the region where major changes occur. In these figures one can observe the existence of the two complex  $\gamma$ - and  $\beta$ -peaks, reported in previous works, and a huge current peak around 240 K at high  $h$  values. This peak is the contribution of the  $\alpha$  and sub- $\alpha$  relaxation processes located at higher temperatures, which positions and intensities are related to the polarization temperature used here ( $T_p = 246$  K). This part of the spectrum at intermediate temperatures will be discussed in the next section when the variations of the high-temperature relaxations will be presented with spectra adequately polarized for their study. The variations of the temperature positions of the current maxima of the  $\gamma$ - and  $\beta$ -relaxations as a function

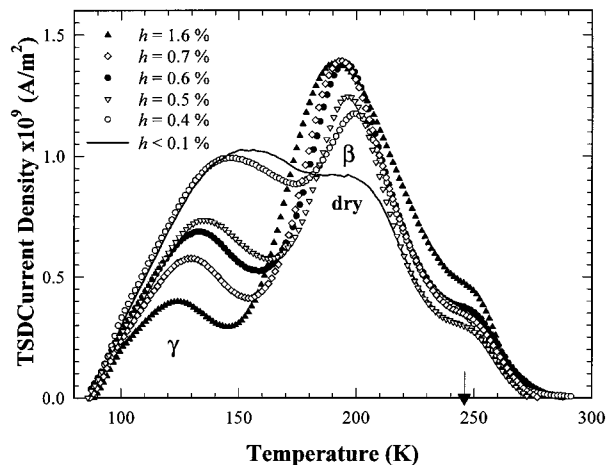


**Figure 2.** Low-temperature TSDC spectra of nylon-6:  $\gamma$ - and  $\beta$ -relaxations with low moisture contents,  $h \leq 1.6\%$ .  $T_p = 246$  K.

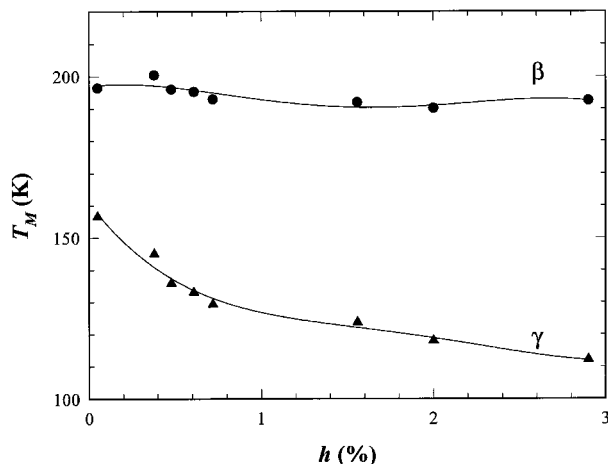


**Figure 3.** Variation of the position of the  $\gamma$ - and  $\beta$ -peaks maxima of nylon-6 as a function of the water content.

of  $h$  are plotted on Figure 3, for  $h < 3\%$ . Higher values of  $h$  have not been included, as the huge contribution of the high-temperature peaks makes difficult any precise determination of the peak positions. In this range, the  $\gamma$ -relaxation shifts to lower temperature,  $T_{M\gamma}$  decreases by 44 K as  $h$  increases, up to 3%, while its intensity also drastically decreases. The  $\beta$ -relaxation has a different behavior; namely, its position shifts within less than 10 K and its intensity increases steeply as  $h$  grows. For  $h \geq 2\%$  the intensity variations observed in Figure 1 are much less significant than in the lowest  $h$  range plotted on Figure 2, and they are strongly affected by the high current overlap of the higher temperature peaks, whose intensity contribution is strongly dependent on  $h$ .

This opposite behavior, namely the increase of the  $\beta$ -relaxation height with  $h$  and the simultaneous intensity decrease of the  $\gamma$ -peak, has also been reported by Frank et al.,<sup>14</sup> and a good qualitative agreement is observed between the intensity variations of the low-temperature TSDC spectra as  $h$  varies. However, some differences between their results and ours are to be noted: First, their TSDC signal is negligible up to 120 K, while in our experiments the current increases drastically from 85 K. The  $\gamma$ -peak reported by these authors is, as a consequence, located at higher temperatures than in our experiments. As for the  $\beta$ -peak, in our runs it is found from 10 to 20 K below the positions observed in Figures 3 and 5 of Frank et al.'s work.<sup>14</sup> A previous TSDC study by Ikeda and Matsuda<sup>12</sup> is difficult to compare to our results as they

show only curves that are strongly affected by the higher temperature peaks due to the high polarization temperature used in their work ( $T_p = 283$  K). In order to be more specific as to the variation of the relaxation parameters and contribution to the polarization of each process present in this very complex TSDC band, the DSA procedure is applied to the whole spectra shown in Figure 2. The temperature dependences for these sub- $T_g$  relaxation modes are taken as Arrhenius as they correspond to localized reorientation processes. As the spectra span a temperature interval of 200 K, the energy window is also taken quite broad, from 0.15 to 0.7 eV, i.e. 40 elementary processes whose contributions are adjusted to best fit the experimental results. In Figure 4 the results of a typical fitting are reported. The excellent agreement reached is quantified by the sum of square residuals,  $\chi^2$ , which is equal to  $1.5 \times 10^{-9}$  (for the TSD current density curve normalized to a polarization equal to 1)<sup>16</sup> or to  $3.3 \times 10^{-21}$  A<sup>2</sup>/m<sup>4</sup> for the current density curve shown in Figure 4(a). The energy histogram shown in Figure 4(b) reports the contribution of each of the 40 energy bins to the total polarization, and the final best  $\tau_{0i}$  values corresponding to each elementary process are plotted in Figure 4(c). It is to be noted that the  $\tau_{0i}$  values resulting from the decomposition of the complex band are within reasonable values and do not take the extremely low values that are often reported in the literature when the decomposition into elementary processes is made by the fractional polarization technique. The energy histograms can now be grouped into 4 energy distributions with Gaussian profiles, labeled  $\gamma_1$ ,  $\gamma_2$ ,  $\beta_1$ , and  $\beta_2$ , which are also drawn on Figure 4(b). As we have already mentioned, the  $\beta_2$  relaxation is incomplete and corresponds to higher temperature modes. In Figure 5 the variation of the contribution to the total polarization of each of these 4 distributions is plotted as a function of the moisture content and the opposite behavior of  $\gamma_2$  and  $\beta_1$  is evident. The variation of the mean energy of each distribution as a function of  $h$  is represented in Figure 6; it is worth noting that these mean energies do not significantly depend on the water content of the material. This result is similar to that reported by Frank et al.<sup>14</sup> after thermal sampling experiments, as they show that the activation energies do not exhibit a dependence of the water content within the accuracy of 0.1 eV. They report for the  $\gamma$ -peak an energy range from 0.3 to 0.5 eV and 0.6 to 0.8 eV for the  $\beta$  peak for  $h \leq 10\%$ ; their values are higher than ours

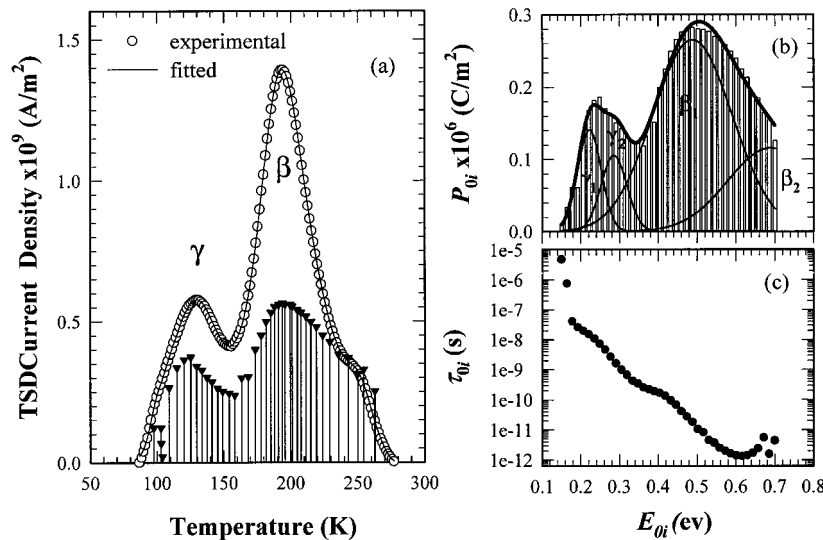


**Figure 4.** DSA results for the  $\gamma$ - and  $\beta$ -peaks of nylon-6,  $h = 0.7\%$ : (a) experimental trace and results of the fitting, with the lines proportional to the contribution of each energy bin; (b) energy histogram; (c) variation of  $\tau_{0i}$  with the energy bin value.

due to the fact that their curves are shifted to higher temperatures. In our case, the energies are constant within 0.02 eV, for  $h < 1.6\%$ , and also lower than those obtained by DS by Pathmanathan et al.<sup>5</sup> in nylon-12. Our analysis was not carried on to higher  $h$  values because of the intense contribution of the sub- $\alpha$  relaxations which will affect seriously any precise analysis of the  $\gamma$ - and  $\beta$ -peaks. The resulting energy dependencies of the

$\tau_{0i}$  values also show some interesting features; there are zones in Figure 4(c) where there is a linear dependence between  $\tau_{0i}$  and  $E_{0i}$ , and this can be interpreted as the existence of compensation laws.

All these reported results help for the assignment of these relaxation modes to different reorientation processes. The nearly independence of the mean energy of the low-temperature modes on the water content also reported in nylon-6,<sup>6,2</sup> and nylon-12<sup>5</sup> indicates that the average environ-

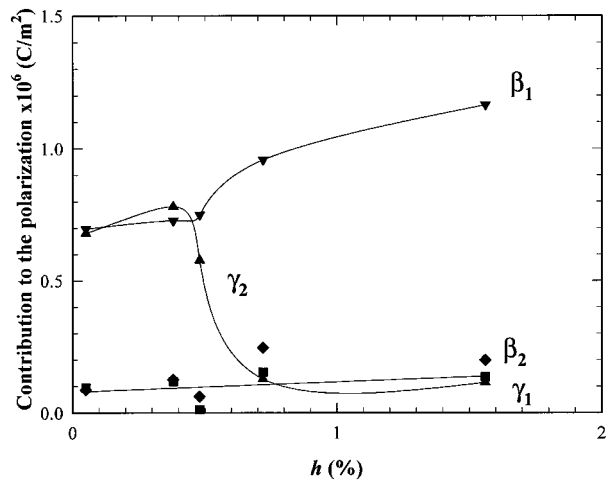


**Figure 5.** Variation for nylon-6 of the contribution to the polarization of each component of the low-temperature band represented in Figure 4(b), as a function of the water content. The lines are drawn to guide the eye; only one line has been traced through the points corresponding to the  $\gamma_1$  and  $\beta_2$  components.

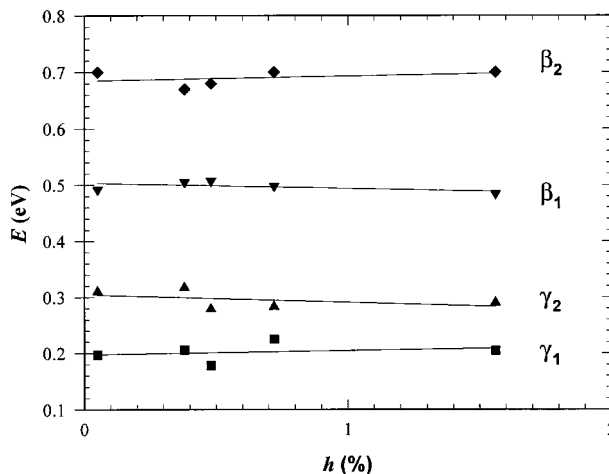


**Figure 6.** Variation for nylon-6 of the mean energy of each component of the low-temperature band represented in Figure 4(b), as a function of the water content.

ment seen by the reorienting entities is not affected by the water molecules. The decrease in the position and intensity of the  $\gamma_2$ -peak as  $h$  increases indicates a diminishing number of orientable dipolar entities as a result of the water sorption. As these effects are most significant in the last steps of the drying process, i.e. the low  $h$  values range, it should correspond to the water molecules that are most difficult to extract by degassing the sample; then, its origin must be related to the firmly bound water proposed by Puffr and Sebenda.<sup>15</sup> These are water molecules that create double hydrogen bonds between neighboring carbonyl groups that were H-bound in the dry material to NH groups. Previous authors<sup>8</sup> have attributed the  $\gamma$ -relaxation to the motion of  $-(CH_2)_n-$  groups which involve the motion of the close amine groups; this interpretation agrees with the new facts encountered here. The firmly bound water would decrease the number of possible reorientable dipoles, interrupting the degree of cooperativity that is necessary and which has been shown to be associated with the existence of a compensation law. The decrease in  $T_{M\gamma}$  might then be related to the shortening of the  $CH_2$  sequences that are able to move. The  $\beta$ -relaxation intensity increase when water is absorbed occurs in the same  $h$  region as the changes just reviewed for the  $\gamma$ -mode. This implies that the explanation for its origin must also be sought in the effect of the firmly bound water whose presence will enhance the intensity of the peak, i.e. increases the number of reorientable entities or their dipolar moment. If this peak is thought to be due to the motion of water-carbonyl groups, this would explain its existence at low  $h$  values, and its intensity increase with  $h$  up to 2%. This attribution of the  $\beta$  relaxation to water-amide complexes agrees with recent interpretations using ac DS<sup>5</sup> and TSDC.<sup>14</sup>

The manifestation of the loosely bound water is seen in the relaxations that occur at intermediate temperatures between the  $\beta$ - and the  $\alpha$ -modes, as they are the first to disappear when the degassing procedure starts. There, the  $H_2O$  molecules are introduced between two amine groups from neighboring chains which were initially H-bound. The  $\beta_2$  distribution was the incomplete manifestation of these processes which are complex and intense as shown in the first curve of Figure 7, which corresponds to  $h = 9.9\%$ . As  $h$  decreases, these sub- $\alpha$  modes intensities also decrease and become a low-temperature tail of the  $\alpha$ -peak without much structure for  $h < 3\%$ . The breaking of the

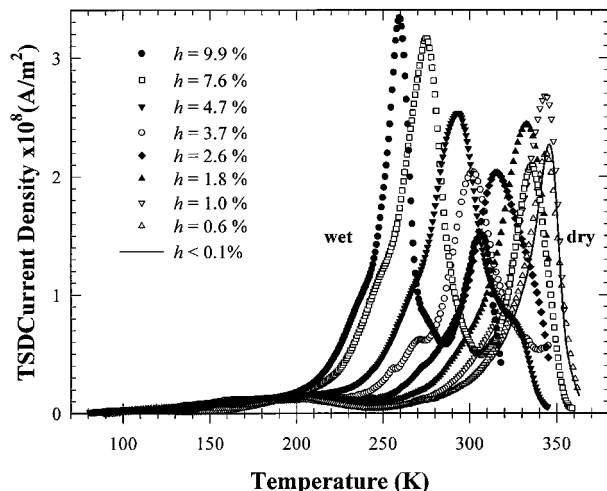


**Figure 7.** High-temperature TSDC spectra of nylon-6:  $\alpha$ - and  $\rho$ -relaxations for the water concentrations indicated in the legend. The polarization temperatures are as follows: ●, 349 K; □, 327 K; ▼, 326 K; ○, 346 K; ◆, 342 K; ▲, 342 K; ▽, 347 K; △, 349 K; —, 349 K.

H bonds existing in the dry material between two amide groups and insertion of water allows movements that were impeded in the first configuration. These water sites only exist in appreciable concentration at high  $h$  values and will decrease rapidly as they are weakly linked to the chain. The clusters that have been proposed as another form of water aggregates in the nearly saturated material could also account for the observed complexity of these intermediate temperature peaks.

#### Glass-Transition Relaxation ( $\alpha$ -Mode)

As it has been shown in Figure 1, there exists at high  $h$  values important contributions to the sample polarization on the high-temperature tail of the  $\beta$ -relaxation which decrease very rapidly as the drying process begins. These contributions are from different origins; the first is due to the existence of depolarization processes at intermediate temperatures, and the second, to the contribution of the  $\alpha$ -relaxation which is shifted toward the  $\beta$ -modes for increasing moisture contents. This is shown in Figure 7, where the spectrum for the most humid sample corresponds to an  $h$  value lower than the saturation value as the sample was degassed for 30 min at room temperature; the resulting highest  $h$  value in this series of experiments is  $h = 9.9\%$ . As the  $\alpha$ -peak is the dielectric manifestation of the glass-rubber transition in nylon-6, it must be associated with the dis-

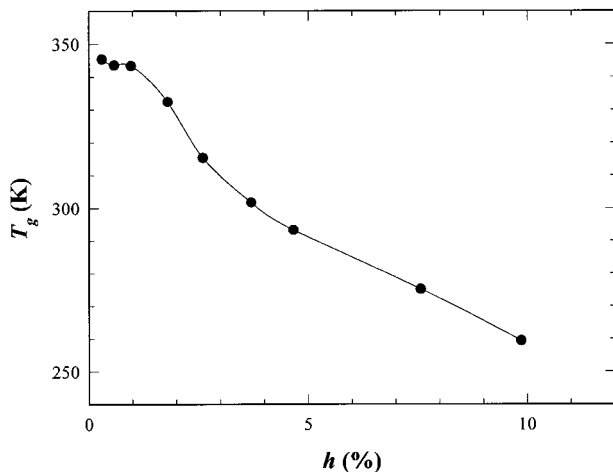


**Figure 8.** Variation of the temperature of the  $\alpha$ -relaxation maximum with the water content.

rupting of H bonds in order to allow long chain segmental motions in the amorphous regions. The important shift of the  $\alpha$ -peak to lower temperatures as the moisture content increases is plotted in Figure 8 and it shows clearly the plasticizing effect of water molecules even in small concentrations. Here a shift from 259 to 345.4 K is observed for  $h$  varying from 9.9% to the dry state. The dry state is reached when the TSDC spectrum does not show any further change after the heating and degassing inherent to the previous TSDC run. Also the strength of the  $\alpha$ -relaxation is varying as expected due both to the variation of the sub- $\alpha$  relaxations, which disappear very rapidly as the drying procedure starts, and to the degree of plasticization induced by the water sorption in the material. The water molecules entering the amorphous phase break the strong H bonds which act as crosslinks, and the chain mobility is increased allowing the long range segmental motions which originate the  $\alpha$ -transition to take place at lower temperatures. The number of orientable dipoles is also affected by the number of crosslinks and existing entanglements as well as by the chain packing in the amorphous regions.

In Figure 8 one observes that  $T_{M\alpha}$  always decreases but at different rates as  $h$  increases, the temperature shift being slower at high  $h$  values. We do not observe here a leveling off for  $T_{M\alpha}$  for high water concentrations as reported by Le Huy and Rault<sup>9</sup> after DMA results on water swollen nylon-6. The shift measured here is in excellent agreement with that reported by Kettle<sup>24</sup> after dilatometric experiments. Rong and Williams<sup>8</sup> also observe in their DMA spectra a peak that

continuously shifts to lower temperatures over the whole concentration range. Additionally, they report a higher temperature peak whose position is not sensitive to  $h$ . By analogy with crosslinking phenomena, where  $(l - n)$  is the crosslinking degree, one can find<sup>9</sup> a critical ratio of sorbed water molecules per amide group in the amorphous region,  $n^*$ , separating the two regimes, which in our case is close to 0.34. For  $n > n^*$  the extra water molecules seem to be less effective for the shifting of  $T_{M\alpha}$  to lower temperatures. If one assumes that the extra moisture is sorbed on the amide sites that are already bound to a water molecule, as the Puffr and Sebenda model<sup>15</sup> proposes, there exists a clustering of water around a concentration of three water molecules per amide group. Following Le Huy and Rault,<sup>9</sup> one can show that the maximum amount of absorbed water is  $3n^*$ , which is observed for the polyamides–water system studied by them by DMA and in agreement with the TSDC results reported here.

The  $\rho$ -peak located at higher temperature than the  $\alpha$ -peak, shown in Figure 7, has been previously reported;<sup>8,11</sup> it is only observed in our study for the samples with  $h \geq 4.7\%$  for which the polarization temperature is well above  $T_{M\alpha}$ . The  $\rho$ -peak is located here at the polarization temperature, and its position and strength should vary with  $T_p$ ; it is attributed to an interfacial polarization relaxation of the Maxwell–Wagner type. The samples for lower water content were not polarized at temperatures higher than 349 K in order to be able to follow the drying process step by step. The  $\rho$ -peak would be in the zone where the sample conductivity starts to increase in the dielectric loss curves of Pathmanathan et al.<sup>5</sup>

When the DSA procedure is applied to the  $\alpha$ -peak to determine the relaxation parameters, the situation is more complicated than in the case of the fitting of the low-temperature peaks. The relaxation time temperature dependence, which is Arrhenius below  $T_g$ , is now described by a VTF expression for  $T \geq T_g$ . This VTF dependence corresponds to a steep reduction in the relaxation times when the sample is heated through the rubber–glass transition temperature region. The non-Debye character of the  $\alpha$ -relaxation exists on both sides of  $T_g$ , and it is interpreted here by a distribution of relaxation times which will be evidenced in the DSA results. In order to avoid the introduction of a parameter to decide the limit where each dependence ceases to be valid, another strategy is followed. The curves obtained when



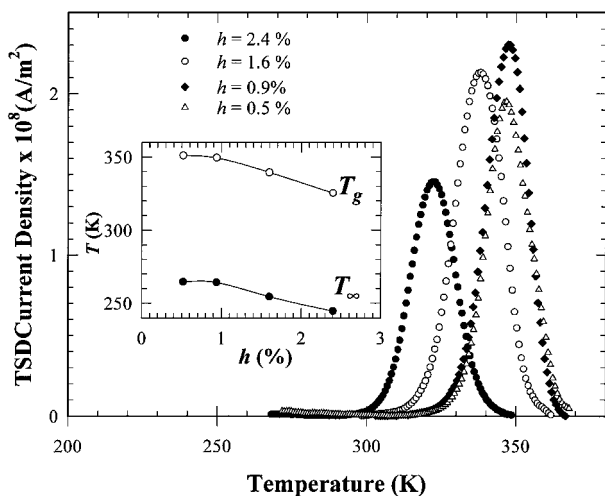


**Figure 9.** TSDC partially discharged spectra of the  $\alpha$ -relaxation of nylon-6 for various water concentrations. The sample was polarized at the temperature of the peak maximum. Insert: Variation of the temperature of the maximum of the  $\alpha$ -relaxation,  $T_g$ , and of the VTF temperature,  $T_\infty$ , with the water content.

the sample is polarized at the maximum of the complex  $\alpha$ -peak are cleaned, i.e., partially discharged to 15 K below  $T_{M\alpha}$ . These clean curves are then analyzed by using a VTF dependence for the relaxation times, as all the Arrhenius components have been minimized. In Figure 9 four clean curves are shown as function of the water content, for  $h < 3\%$ . In the insert of this figure the variation of the peak maximum and of the VTF temperature,  $T_\infty$ , are plotted vs.  $h$ . These  $T_\infty$  values are obtained from the best fit reached for each clean curve with the DSA. In Figure 10 the results of the fitting corresponding to the sample with  $h = 1.6\%$  are plotted. A general feature of these fittings, obtained by adjusting the parameters of 13 elementary curves, is the excellent agreement reached as shown by the sum of square residual values,  $\chi^2 = 1.3 \times 10^{-8}$ , for the curve whose total polarization has been normalized to unity;<sup>16</sup> the energy goes from 0.04 to 0.15 eV, and the range of the  $\tau_{0i}$  values is totally acceptable. For each  $h$  value, a  $T_\infty$  value is obtained and its variation is a decreasing function of  $h$ . The ratio  $T_{M\alpha}/T_\infty$  is constant and equal to 1.33 in agreement with the value calculated by Adam and Gibbs<sup>23</sup> for widely differing materials. The energy corresponding to the most intense bin of the energy histogram varies from 0.063 to 0.080 eV as  $h$  decreases from 2.4% to 0.5%. Pathmanathan et al.<sup>5</sup> determined in dry nylon-12 the  $B$  constant in the VTF expression for the frequency ( $f_m = A \exp[-B/(T - T_\infty)]$ )

to be equal to 505.4 K which is equivalent to 0.044 eV ( $E = kB$ ) for the VTF energy defined in eq. (3). The determination of this relaxation energy allows the estimate of the fractional free volume trapped in the amorphous zones of the material. The estimate is made by calculating the expansion coefficient as  $k/E$ , which is the inverse of the VTF energy, and computing the resulting fractional volume as  $\nu_f = \alpha(T_M - T_\infty)$ . This results in a fractional volume varying from 9% in the nearly dry sample to 11% for  $h = 2.4\%$ . This small variation is in the opposite direction to that observed in nylon-12 by Pathmanathan et al.,<sup>5</sup> where a decrease in volume was assumed to explain the observed density increase as the water concentration grows. Our results do not seem to indicate that in nylon-6 the introduction of tightly bound water molecules makes the chain packing more efficient than in its absence. The introduction of water molecules if correctly described by the mechanism proposed by Puffr and Sebenda,<sup>15</sup> even if it removes the steric requirements for the formation of H bonds, still requires slightly more space to accommodate the strongly linked water so as the chains are less closely packed when the sample is swollen.

## CONCLUSIONS

The detailed study of the  $\gamma$ -,  $\beta$ -, and  $\alpha$ -relaxations by TSDC techniques in the presence of sorbed water molecules shows several remarkable features. Water increases the  $\beta_1$ - and decreases the  $\gamma_2$ -relaxation strength which also shifts to lower temperatures as  $h$  increases. The reorienting energies of these two low-temperature processes are almost constant for  $h$  values up to 2%. The tightly bound water molecules which create double H bonds between neighboring CO groups are responsible for these variations. The  $\gamma$ -relaxation is attributed to the motion of the amine groups accompanied by the  $(\text{CH}_2)_n$  groups while the  $\beta$ -peak is originated by water-carbonyl groups. The plasticization effect of water affects the position of the  $\gamma$ -peak in these localized modes. As for the loosely bound water, it gives rise to at least two intense and overlapping relaxation processes in the intermediate temperature region, between the  $\beta$ - and the  $\alpha$ -peaks. These modes disappear easily by degassing the sample at room temperature.

At higher temperatures the  $\alpha$ -relaxation is the cooperative mode that is most affected by the water sorption. The peak is shifted to higher temper-

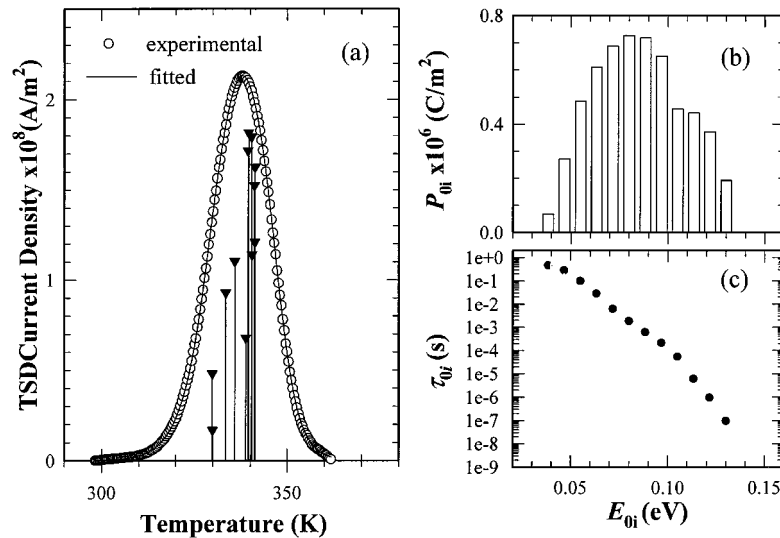


**Figure 10.** DSA results for the  $\alpha$ -peak of nylon-6,  $h = 1.6\%$ : (a) experimental trace and results of the fitting, with the lines proportional to the contribution of each energy bin; (b) energy histogram; (c) variation of  $\tau_{0i}$  with the energy bin value.

atures ( $\Delta T = 86$  K) as the drying procedure takes place and its strength is decreased. The VTF temperature and energy decrease following the variation of  $T_g$  in the first steps of the sorption process showing the plasticization effect by water molecules which slightly increase the free volume in the material.

This work is part of Project NM-012, of the Programa de Nuevas Tecnologías, and of Project DID G-15; we are deeply indebted to the Consejo Nacional de Investigaciones Científicas y Tecnológicas, CONICIT, and to the Decanato de Investigación y Desarrollo for their financial support. The collaboration of A. Bello and M. Grimau is gratefully acknowledged.

## REFERENCES AND NOTES

1. R. H. Boyd, *J. Chem. Phys.*, **30**, 1276 (1959).
2. H. W. Starkweather, Jr. and J. R. Barkley, *J. Polym. Sci.: Polym. Phys. Ed.*, **19**, 1211 (1981).
3. D. W. McCall and E. W. Anderson, *J. Chem. Phys.*, **32**, 237 (1960).
4. K. Pathmanathan and G. P. Johari, *J. Chem. Soc., Faraday Trans.*, **91**, 337 (1995).
5. K. Pathmanathan, J. Y. Cavaille, and G. P. Johari, *J. Polym. Sci. B*, **30**, 341 (1992).
6. A. E. Woodward, J. A. Sauer, C. W. Deeley, and D. E. Kline, *J. Colloid Sci.*, **12**, 363 (1957).
7. S. Kapur, C. E. Rogers, and E. Baer, *J. Polym. Sci.: Polym. Phys. Ed.*, **10**, 2297 (1972).
8. S. Rong and H. L. Williams, *J. Appl. Polym. Sci.*, **30**, 2575 (1985).
9. H. M. Le Huy and J. Rault, *Polymer*, **35**, 136 (1994).
10. J. Varlet, J. Y. Cavaille, and J. Perez, *J. Polym. Sci.: Polym. Phys. Ed.*, **28**, 2691 (1990).
11. D. Chatain, P. Gautier, and C. Lacabanne, *J. Polym. Sci.: Polym. Phys. Ed.*, **11**, 1631 (1973).
12. S. Ikeda and K. Matsuda, *Jpn. J. Appl. Phys.*, **19**, 855 (1980).
13. J. L. Gil-Zambrano and C. Juhasz, *IEEE Trans. Elect. Ins.*, **24**, 635 (1989).
14. B. Frank, P. Frübing, and P. Pissis, *J. Polym. Sci.: Polym. Phys. Ed.*, **34**, 1853 (1996).
15. R. Puffr and J. Sebenda, *J. Polym. Sci. C*, **16**, 79 (1967).
16. M. Aldana, E. Laredo, A. Bello, and N. Suarez, *J. Polym. Sci.: Polym. Phys. Ed.*, **32**, 2197 (1994).
17. E. Laredo, M. Grimau, A. Müller, A. Bello, and N. Suarez, *J. Polym. Sci., Part B: Polym. Phys.*, **34**, 2863 (1996).
18. N. Suarez, E. Laredo, A. Bello, and J. Kohn, *J. Appl. Polym. Sci.*, **63**, 1457 (1997).
19. M. A. Gomez, C. Marco, J. M. G. Fatou, N. Suarez, E. Laredo, and A. Bello, *J. Polym. Sci., Part B: Polym. Phys.*, **33**, 1259 (1995).
20. N. Suarez, E. Laredo, A. Bello, M. A. Gomez, C. Marco, and J. M. G. Fatou, *Polymer*, **37**, 3207 (1995).
21. E. Laredo, N. Suarez, A. Bello, and L. Marquez, *J. Polym. Sci., Part B: Polym. Phys.*, **34**, 641 (1996).
22. M. H. Cohen and G. S. Grest, *Phys. Rev. B*, **24**, 4091 (1981).
23. G. Adam and J. H. Gibbs, *J. Chem. Phys.*, **43**, 139 (1965).
24. G. J. Kettle, *Polymer*, **18**, 742 (1977).